Journal of Experimental Botany, Vol. 59, No. 13, pp. 3523–3531, 2008
doi:10.1093/jxb/ern202 Advance Access publication 13 August, 2008
This paper is available online free of all access charges (see http://jxb.oxfordjournals.org/open_access.html for further details)

Journal of Experimental Botany
www.jxb.oxfordjournals.org

RESEARCH PAPER

An isoform of *Arabidopsis* myosin XI interacts with small GTPases in its C-terminal tail region

Kohsuke Hashimoto[1], Hisako Igarashi[2], Shoji Mano[3], Chikako Takenaka[4], Takashi Shiina[4], Masatoshi Yamaguchi[2], Taku Demura[2], Mikio Nishimura[3], Teruo Shimmen[1] and Etsuo Yokota[1,*]

[1] *Department of Life Science, Graduate School of Life Science, University of Hyogo, Harima Science Park City, Hyogo 678-1279, Japan*

[2] *RIKEN Plant Science Center, 1-7-22 Suehiro-cho Turumi-ku, Yokohama, Kanagawa 230-0045, Japan*

[3] *Department of Cell Biology, National Institute for Basic Biology, Okazaki 444-8585, Japan*

[4] *Graduate School of Human Environmental Sciences, Kyoto Prefectural University, Nakaragi-cho, Shimogamo, Sakyo-ku, Kyoto 606-8522, Japan*

Received 6 March 2008; Revised 7 July 2008; Accepted 8 July 2008

Abstract

Myosin XI, a class of myosins expressed in plants is believed to be responsible for cytoplasmic streaming and the translocation of organelles and vesicles. To gain further insight into the translocation of organelles and vesicles by myosin XI, an isoform of *Arabidopsis* myosin XI, MYA2, was chosen and its role in peroxisome targeting was examined. Using the yeast two-hybrid screening method, two small GTPases, AtRabD1 and AtRabC2a, were identified as factors that interact with the C-terminal tail region of MYA2. Both recombinant AtRabs tagged with His bound to the recombinant C-terminal tail region of MYA2 tagged with GST in a GTP-dependent manner. Furthermore, AtRabC2a was localized on peroxisomes, when its CFP-tagged form was expressed transiently in protoplasts prepared from *Arabidopsis* leaf tissue. It is suggested that MYA2 targets the peroxisome through an interaction with AtRabC2a.

Key words: AtRabC2a, AtRabD1, myosin XI, MYA2, peroxisome.

Introduction

Myosin is a molecular motor protein, which acts on actin filaments. It is composed of light and heavy chains which are divided into head, neck, and tail regions. The head region binds to actin filaments and moves along them, dependent upon ATP hydrolysis. On the basis of the primary structure of this region, myosin is classified into at least 24 classes (Foth *et al*., 2006). Light chains, in many cases calmodulin, bind to the neck region. The C-terminal tail region is diverse in size and primary structure among myosin classes, and is inferred to determine the physiological function of each class of myosin in cells.

Only three classes of myosin, VIII, XI, and XIII, have been identified in plant cells (Reichelt and Kendrick-Jones, 2000; Sellers, 2000). In *Arabidopsis thaliana*, 17 myosins have been identified by searching the database. Among them, four belong to class VIII and 13 to class XI (Reichelt and Kendrick-Jones, 2000; Reddy and Day, 2001). Pharmacological studies, using actin-depolymerizing drugs and myosin inhibitors, have demonstrated that most organelles, including endoplasmic reticulum (E Yokota, S Ueda, K Tamura, H Orii, S Uchi, S Sonobe, I Hara-Nishimura, and T Shimmen, unpublished data), mitochondria (Logan and Leaver, 2000; Van Gestel *et al*., 2002), chloroplasts (Wada *et al*., 2003; Paves and Truve, 2007), plastids (Kwok and Hanson, 2003), peroxisomes (Jedd and Chua, 2002; Mano *et al*., 2002; Mathur *et al*., 2002; Collings *et al*., 2003), vacuoles (Higaki *et al*., 2006), and Golgi (Boevink *et al*., 1998; Nebenfuhr *et al*., 1999) move, or are translocated, using the actin–myosin system. Among these organelles, mitochondria and plastids in maize root cells (Wang and Pesacreta, 2004), mitochondria in tobacco pollen tubes (Romagnoli *et al*., 2007) and endoplasmic reticulum in tobacco cultured BY-2 cells (E Yokota, S Ueda, K Tamura, H Orii, S Uchi, S Sonobe,

* To whom correspondence should be addressed: E-mail: yokota@sci.u-hyogo.ac.jp

I Hara-Nishimura, and T Shimmen, unpublished data), immunostained with an antibody against myosin XI. It has previously been shown that an isoform of myosin XI, MYA2, was co-localized with peroxisomes and, thus far, unidentified vesicles in *Arabidopsis* by immunostaining with a specific antibody against MYA2 tail region (Hashimoto *et al*., 2005). Furthermore, the transport and movement of Golgi, mitochondria, and peroxisomes were suppressed or modified by the knockout of certain isoforms of myosin XI in tobacco (Avisar *et al*., 2008) and *Arabidopsis* cells (Peremyslov *et al*., 2008). These studies indicate the involvement of myosin XI in the movement of various types of organelles in plant cells. When a fluorescence-protein-tagged tail region of several myosin XI isoforms was expressed in tobacco, onion (Reisen and Hanson, 2006), and *Arabidopsis* cells (Li and Nebenfuhr, 2007), Golgi and peroxisomes were tagged. In some cases, the movement of these organelles and mitochondria was reported to be suppressed or modified by the expression of the tail region (Avisar *et al*., 2008; Peremyslov *et al*., 2008). These results suggest that myosin XI is associated with organelles through its tail region. The tail regions of myosin XI isoforms are divided into two short subdomains, with organelles associating with either of them independently (Li and Nebenfuhr, 2007). Interestingly, a full-length tail or a long tail isoform, containing the coiled-coil domain of myosin XI, does not target specific organelles or bind to unknown organelles. Based on this evidence, it was suggested that the organelle targeting of each myosin XI isoform is selected and regulated in the cells, and it appears likely that myosin XI isoforms have a mechanism for recognizing and selecting organelles in their tails.

In animal and yeast cells, it is known that small GTPases, Rab proteins, interact with class V myosin, which is functionally and structurally similar to myosin XI, and are important in organellar and vesicular targeting. In budding yeast, a Rab protein, Ypt11p, functions in mitochondrial distribution into the developing bud through the interaction with the tail region of myosin V, Myo2p (Itoh *et al*., 2002). In mammalian cells, myosin Vb regulates the plasma membrane recycling system through its association with Rab11a and Rab11-family-inertacting protein-2 (Rab11-FIP2; Lapierre *et al*., 2001; Hales *et al*., 2002). Furthermore, the formation of a complex between Rab27a, melanophilin and myosin Va, is required for normal melanosome transport in the melanophore (Storm *et al*., 2002; Kuroda *et al*., 2003).

In the present study, small GTPase Rabs, AtRabD1 and AtRabC2a, were identified as interacting factors with the tail region of MYA2 by yeast two-hybrid screening. An *in vitro* binding assay showed that the tail region of MYA2 binds to these AtRab proteins in a GTP-dependent manner. Furthermore, AtRabC2a was localized on peroxisomes in protoplasts prepared from *Arabidopsis* leaf tissue. These results suggested that MYA2 is targeted to peroxisomes through an interaction with AtRabC2a.

Materials and methods

Yeast two-hybrid screening

Truncated MYA2 tails were amplified by RT-PCR with total RNA isolated from leaves of 4-week-old plants by an RNeasy Plant Kit (Qiagen, Valencia, CA, USA). The PCR amplification products were subcloned into pENT/D/TOPO vector (Invitrogen, Carlsbad, CA), and then integrated into a pBD-GAL4-GWRFC derived from pBD-GAL4 Cam vector (Stratagene, LA Jolla, CA) by LR clonase (Invitrogen). A yeast AH109 strain (Clontech) was co-transfected with MYA2(aa1049-aa1505)/pBD-GAL4-GWRFC and 300 μg of an *Arabidopsis* root cDNA plasmid library which was constructed in pAD-GAL4-GWRFC, derived from a pAD-GAL4-2.1 vector (Stratagene), and plated on the selection media containing 5 mM 3-aminotriazole but lacking leucine, tryptophan, and histidine. After 2 weeks of growth, positive colonies were picked up and regrown on the selection media. Significant growth on the selection media indicated a positive interaction. The plasmids were then recovered from the colonies using a Zymoprep Kit (Zymo Research, Orange, CA) and introduced into an *E. coli* TOP10 strain (Invitrogen) with selection by ampicillin. A DNA sequencer (ABI PRISM 3000) was used for sequence analysis. For the examination of Rab binding sites in the MYA2 tail, the yeast AH109 strain was co-transfected with Rab/pAD-GAL4-GWRFC and one of the various truncated MYA2/pBD-GAL4-GWRFC, then plated on the control media. After 4 d growth, the colonies were regrown on the selection and control media. To confirm no positive interactions by self-activation, the co-transfection with MYA2 tail bait and empty prey vectors or Rab prey and empty bait vectors were performed. In addition, co-transfection with pBD-wt and pAD-wt (Stratagene) or empty bait and empty prey vectors were performed for the control experiments.

Isolation of recombinant proteins

MYA2 tail (aa1049–aa1505 or aa1049–aa1450) in a pENT/D-TOPO vector was amplified using a forward primer with *Eco*R1 and a reverse primer with *Xho*1 and cloned into a pGEX4T-1 vector (Amersham) using their restriction sites by a DNA ligation kit ver.2.1 (TaKaRa). The full-length cDNAs of AtRabD1 and AtRabC2a were also amplified by RT-PCR with total RNA isolated from leaves of 4-week-old plants using an RNeasy Plant Kit. PCR amplification products were subcloned into the pENT/D-TOPO vector (Invitrogen), and then transformed into a pDEST17 vector (Invitrogen) by LR clonase (Invitrogen). MYA2 tail/pGEX4T-1 and Rab/pDEST17 were introduced into *E. coli* BL21pLysS cells (Invitrogen). AtRabD1 and AtRabC2a fused with His×6 tag at their N-terminal regions were purified through a Ni-Sepharose column according to the manufacturer's protocol (Amersham Bioscience). Rab proteins were dialysed against NEMP solution containing 60 mM NaCl, 2 mM EGTA, 1 mM $MgCl_2$, 0.5 mM DTT, 50 μg ml^{-1} leupeptin, 0.5 mM PMSF, and 20 mM PIPES-KOH (pH 7.0) and used for *in vitro* binding assays. Each MYA2 tail protein fused with GST at its N-terminal region in the crude extract from *E. coli* was adsorbed on glutathione-Sepharose beads and then washed according to the manufacturer's protocol (Amersham). Beads were equilibrated with EMP solution containing 2 mM EGTA, 1 mM $MgCl_2$, 0.5 mM DTT, 50 μg ml^{-1} leupeptin, 0.5 mM PMSF, and 20 mM PIPES-KOH (pH 7.0) and then suspended in EMP solution supplemented with 0.05% BSA.

In vitro *binding assay*

The same batch of beads coated with MYA2 tails was used to analyse the binding of each His6-taged Rab protein. 39 μl of each

Rab protein (30 μg ml^{-1}) and 1 μl of 80 mM GTP or deionized water was added to 40 μl of the suspension of beads (15 μl of void volume) in a microcentrifuge tube. The mixture was gently suspended at 3 min intervals for 20 min at room temperature. After centrifugation at 500 rpm at room temperature, the supernatant was carefully discarded, and 65 μl of NEMP solution was added to the pellet. During washing, 300 μl of NEMP solution with or without 1 mM GTP was added to the pellet. After centrifugation, one aliquot of pellet was pooled, while a second aliquot of pellet was washed with 300 μl of NEMP solution and then centrifuged. Each pellet was subjected to SDS-PAGE using a 12% gel by the method of Laemmli (1970). After staining with Coomassie brilliant blue (CBB), the intensity of each band of Rab proteins was measured using a densitometer (Densito-pattern analyser model no. EPA-3000, Cosmo Bio. Co. Ltd., Tokyo).

Leaf protoplast preparation

A transgenic *Arabidopsis* expressing the GFP-tagged peroxisomal targeting signal peptide 1 (GFP-PTS1; Mano *et al*., 2002) was used for examining positional and distributional relationships between peroxisomes and AtRab proteins. *Arabidopsis* seedlings were grown on Murashige and Skoog plates at 22 °C. Rosette leaves of 2-week-old plants were cut into 1–2 cm sections with a razor blade. Samples were digested for about 3 h in an enzyme solution [1.5% cellulase R-10 (Onozuka, Tokyo, Japan), 0.4% macerozyme R10 (Yakult, Tokyo, Japan), 0.4 M mannitol, 20 mM KCl, 10 mM $CaCl_2$, 0.1% BSA, and 20 mM MES (pH 5.7)] whilst being shaken at 40 rpm at 23 °C. The mixture was filtered with a 50 μm nylon mesh. After centrifugation at 100 *g* for 3 min, the pellet was suspended in a solution containing 0.4 M mannitol, 15 mM $MgCl_2$ and 4 mM MES (pH 5.7).

Transient expression in Arabidopsis *leaf protoplasts*

A full-length cDNA of AtRabC2a or AtRabD1 was fused to the C-terminus of CFP controlled by the 35S CaMV promoter by GATEWAY technology. The construct was introduced into protoplasts by a PEG-mediated transformation method (Sheen, 2002; http://genetics.mgh.harvard.edu/sheenweb/). Protoplasts expressing the fusion protein were observed under an Olympus BX60 fluorescence microscope equipped with filters for GFP (U-MNIBA, Olympus) and CFP fluorescence (U-MCFPHQ, Olympus). Images were taken with a digital camera (DP 70, Olympus) controlled by Aquacosmos software (Hamamatsu Photonics). Unmixed images with the two types of fluorescence were subsequently acquired by processing with U9677 Multiband Imaging software (Hamamatsu Photonics).

Results

Identification of AtRab proteins as interacting factors with the C-terminal tail region of MYA2

To investigate the function of the MYA2 tail, potential factors that interact with the C-terminal tail region of MYA2 were searched using a two-hybrid screening method. An *Arabidopsis* root cell cDNA library with the tail region of MYA2, aa1049–aa1505 (f1), lacking the coiled-coil domain, as shown schematically in Fig. 1A was screened. After screening 1.2×10^6 clones, DNA fragments encoding AtRabD1 and AtRabC2a, members of the small GTPase Rab family, were identified. To determine the region in the MYA2 tail responsible for the interaction with each AtRab, their interaction with a series of deletion forms of the MYA2 tail, aa1049–aa1450 (f2 in Fig. 1A), aa900–aa1221 (f3 in Fig. 1A), in which the coiled-coil domain was included, and aa1195–aa1505 (f4 in Fig. 1A) was examined. The association of each AtRab to each truncation of the MYA2 tail is summarized in Fig. 1B. AtRabD1 interacted with a truncation of MYA2 tail, aa1049–aa1450 (f2) lacking 55 amino acids in the C-terminus, but not with aa900–aa1221 (f3) containing only the N-terminal region, and aa1195–aa1505 (f4), lacking the N-terminus. These results suggest that the boundary region between aa1195 and aa1221 in the MYA2 tail is important for the interaction with AtRabD1. By contrast, AtRabC2a interacted only with a full-length MYA2 tail (f1), but not with its truncated forms, where 55 amino acids from the C-terminus or 146 amino acids from N-terminus were deleted. Therefore, both tail termini appear to be necessary for the interaction with AtRabC2a.

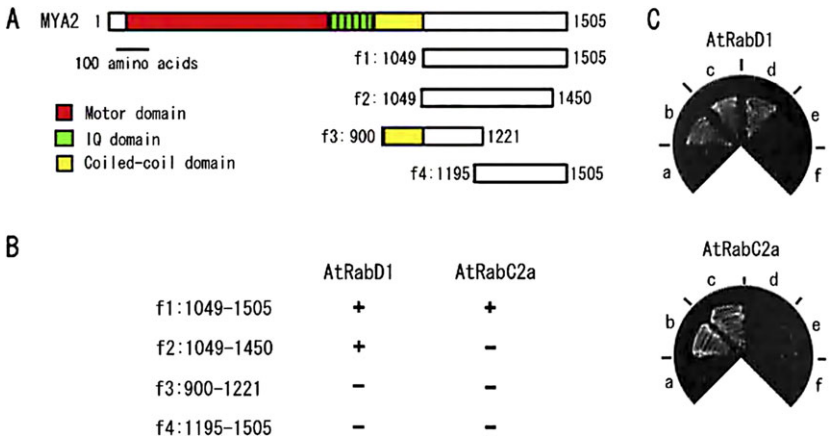

Fig. 1. Interaction of AtRabD1 and AtRabC2a with truncated MYA2 tails in the yeast two-hybrid method. (A) A diagram of the tail regions of MYA2, fragment 1 to 4 (f1 to f4), tested for the interaction with AtRabD1 and AtRabC2a. (B) Interaction of AtRabD1 or AtRabC2a with each truncated form of the MYA2 tail (f1 to f4): + or – indicates a negative or positive interaction, respectively. (C) Photographs of yeast co-transfected with truncations of MYA2 tail (MYA2 f1 (c), MYA2 f2 (d) MYA2 f3 (e), MYA2 f4 (f)) as bait and AtRabD1 (upper) or AtRabC2a (bottom) as prey on the selection media. Negative or positive control interaction is (a) or (b), respectively. Significant growth indicated a positive interaction.

Interaction of recombinant MYA2 tail proteins with recombinant AtRabD1 and AtRabC2a in vitro

Like other regulatory GTPases, the Rab protein interchanges between the active GTP-bound and inactive GDP-bound forms, each of which have different conformations from the other (Ali and Seabra, 2005). The GTP-bound form of the Rab protein interacts with effector proteins rendering it catalytically active. It was examined whether AtRabD1 and AtRabC2a interact with MYA2 tails at the protein level, and whether any interaction is GTP dependent. AtRabD1 (lane a in Fig. 2A) and AtRabC2a (lane b in Fig. 2A) fused with His6, and MYA2 tails, aa1049–aa1505 (MYA2 tail 1; lane c in Fig. 2A) and aa1049–aa1450 (MYA2 tail 2; lane d in Fig. 2A), fused with GST, were expressed in *E. coli* and purified by affinity chromatography as described in the Materials and methods. Each MYA2-tail recombinant protein fused with GST was bound to glutathione Sepharose beads, and was used for an *in vitro* binding assay using a pull down assay. Beads without the MYA2 tail bound to them were used as a control.

First, the interaction of both recombinant AtRab proteins with the MYA2 tail 1 was examined. In the absence of GTP (lane b in Fig. 2B), the amount of both His6-AtRab proteins, which recovered in pellets with beads coated with the MYA2 tail 1, appeared to be same as that recovered with control beads (lane a in Fig. 2B). However, the amount of both AtRab proteins in pellets with MYA2 tail 1 coated beads was increased by the addition of GTP (lane c in Fig. 2B). Densitometric band analysis of AtRab protein in the pellet showed that the amount of AtRabD1 (white bars in Fig. 3A) and AtRabC2a protein (shaded bars in Fig. 3A) bound to the MYA2 tail 1 coated beads in the presence of GTP (+GTP in Fig. 3A) was 2.6-fold and 1.7-fold, respectively, larger than that in the absence of GTP (–GTP in Fig. 3A) or that bound to the control beads in the presence of GTP, indicating that both recombinant AtRab proteins had an ability to bind to the MYA2 tail 1 in a GTP-dependent manner and that the affinity of AtRabD1 for the MYA2 tail 1 was higher than that of AtRabC2a.

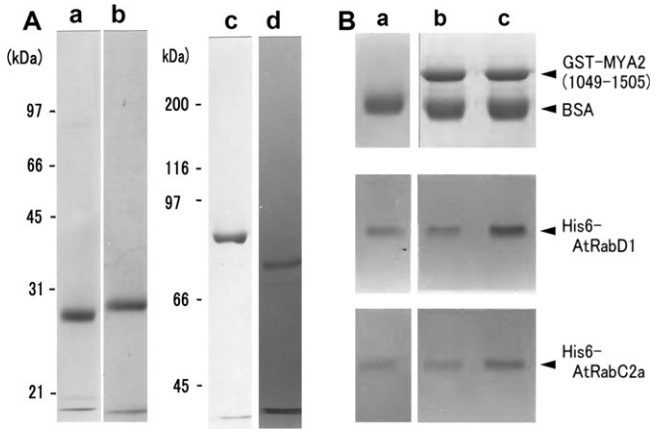

Fig. 2. Recombinant proteins (A) and *in vitro* binding assay (B). (A) SDS-PAGE of His6-AtRabD1 (a), His6-AtRabC2a (b), MYA2 tail 1, aa1049-aa1505, fused with GST (c), and MYA2 tail 2, aa1049-aa1450, fused with GST (d). The molecular masses (kDa) of standard proteins in SDS-PAGE of (a), (b), (c) and (d) are indicated on the left of lanes (a) and (c), respectively. (B) *In vitro* binding assay using MYA2 tail 1. (a) Pellets with control beads without the adsorption of GST-MYA2 tail 1 in the presence of GTP. (b) Pellets with MYA2 tail 1 coated beads in the absence of GTP. (c) Pellets with MYA2 tail 1 coated beads in the presence of GTP. Each bead was mixed with His6-AtRabD1 or His6-AtRabC2a. After centrifugation, the pellets were subjected to SDS-PAGE. Upper, middle, and lower panels, MYA2 tail 1, His6-AtRabD1, and His6-AtRabC2a in the pellet, respectively. Bovine serum albumin (BSA) was added to the mixture for preventing the non-specific binding of AtRab proteins to beads.

Next, the interaction of both AtRab proteins with the MYA2 tail 2 (Fig. 4A) was examined. The amount of AtRabD1 protein (white bars in Fig. 4A) bound to MYA2 tail 2 coated beads in the presence of GTP (+GTP in Fig. 4A) was 1.6-fold larger than that in the absence of GTP (–GTP in Fig. 4A) or that bound to the control beads in the presence of GTP, indicating that this AtRab protein was also able to associate with the MYA2 tail 2 in a GTP-dependent fashion. However, the amount of AtRabC2a protein (shaded bar in Fig. 4A) bound to the beads coated with the MYA2 tail 2 in the presence of GTP (+GTP in Fig. 4A) was similar to that in the absence of GTP (–GTP in Fig. 4A) or that bound to the control beads. Thus, AtRabC2a protein did not associate with the MYA2 tail 2 even in the presence of GTP, supporting the results of the two-hybrid analysis.

However, these recombinant AtRab proteins readily dissociated from the MYA2 tail 1 (Fig. 3B; white bars and shaded bars for AtRabD1protein and AtRabC2a protein, respectively) or tail 2 (Fig. 4B) adsorbed to beads by washing with a solution containing GTP. These results indicate that AtRabD1 and AtRabC2a protein tagged with His6 interacted weakly with the MYA2 tails fused with GST in a GTP dependent manner.

Co-localization of transiently expressed AtRabC2a with peroxisomes

Next, the intracellular localization of each AtRab protein was examined in relation to peroxisomes in *Arabidopsis* cells, in which peroxisomal targeting signal 1 (PTS1) tagged with GFP was stably expressed (Mano *et al*., 2002). Since the primary structures of AtRab proteins show high levels of homology with isoforms in subgroups (A and B for AtRab isoforms belonging to C and D subgroups, respectively, in Fig. 5), it was considered that it was not feasible to make an antibody against AtRabC2a or AtRabD1. Hence, the localization of AtRabD1 or AtRabC2a protein was evaluated by the transient expression of their CFP-fused forms in leaf cell protoplasts. Dot signals of CFP-AtRabC2a (Fig. 6B) generally overlapped with GFP-tagged PTS1 signals, peroxisomes (Fig. 6A). When a protoplast not transformed with CFP-tagged AtRabC2a (Fig. 6C) was

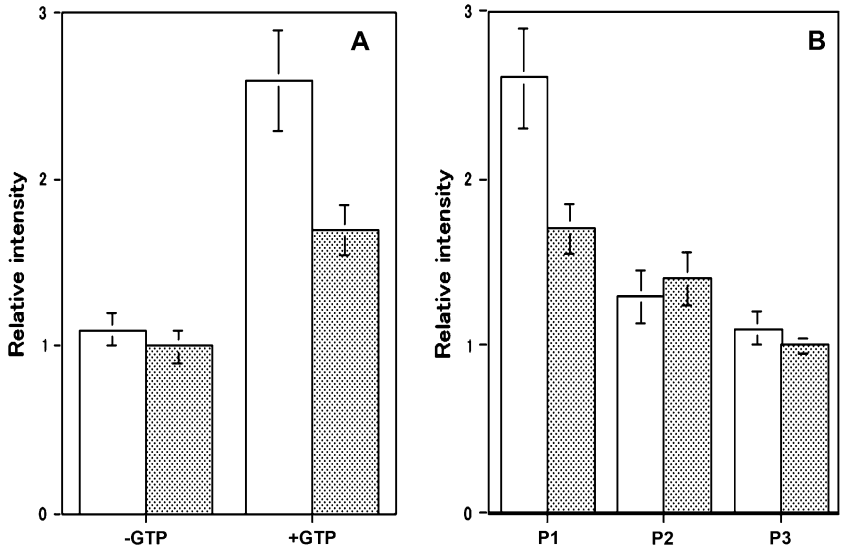

Fig. 3. Quantitative analysis of His6-AtRab proteins bound to MYA2 tail 1 fused with GST in *in vitro* binding assays. (A) Binding of His6-AtRab proteins to MYA2 tail 1 coated beads in the absence (–GTP) or presence of GTP (+GTP). White and shaded bars show the amount of His-AtRabD1 and His-AtRabC2a, respectively, in the pellet with MYA2 tail 1 coated beads. Each AtRab protein was mixed with beads in the absence or presence of GTP, or with control beads in the presence of GTP. After centrifugation, the pellets were subjected to SDS-PAGE, and the intensity of each AtRab protein band was determined. The intensities are shown as a relative value to that of control beads. Averages ±SD from three separate experiments are plotted. (B) Dissociation of His-AtRab proteins from MYA2 tail 1 by washing with a buffer containing GTP. White and shaded bars showed the amount of His-AtRabD1 and His-AtRabC2a, respectively, in the pellets with MYA2 tail 1 coated beads. Each His-AtRab protein was mixed with MYA2 tail 1 coated beads in the presence or absence of GTP. The beads were washed twice as described in the Materials and methods. The amounts of each AtRab protein recovered in the first pellets (P1), second pellets (P2), and third pellets (P3) are given relative to that of pellets in the absence of GTP. Averages ±SD from three separate experiments are plotted.

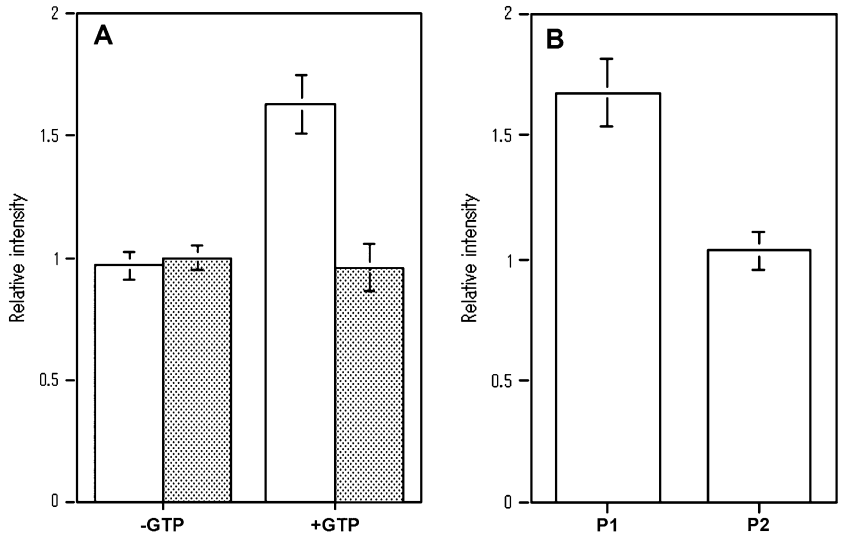

Fig. 4. Quantitative analysis of His6-AtRab proteins bound to MYA2 tail 2 fused with GST in *in vitro* binding assays. (A) Binding of His6-AtRab proteins to MYA2 tail 2 coated beads in the absence (–GTP) or presence of GTP (+GTP). White and shaded bars showed the amount of His-AtRabD1 and His-AtRabC2a, respectively, in the pellet with MYA2 tail 2 coated beads. Each His-AtRab protein was mixed with beads in the absence or presence of GTP, or with control beads in the presence of GTP. The amounts of each AtRab protein recovered with beads were determined and are shown as described in the legend to Fig. 3A. Averages ±SD from four separate experiments are plotted. (B) Dissociation of His6-AtRabD1 from MYA2 tail 2 by washing with a buffer containing GTP. His6-AtRabD1 was mixed with MYA2 tail 2 coated beads in the presence or absence of GTP. Washing was performed by the same method as described in the legend to Fig 3B. P1 and P2 show the amounts of His-AtRabD1 recovered in first and second pellets, respectively. Averages ±SD from four separate experiments are plotted.

observed through a CFP filter, few signals were detected (Fig. 6D). Conversely, diffuse signals of CFP-tagged AtRabD1 (Fig. 6F, H) were observed throughout the cytoplasm, and peroxisomes appeared to be embedded with these signals. In some cases, the GFP-labelled peroxisome signals did not overlap with those of AtRabD1 (white arrows in Fig. 6H). However, at present, it is not possible to determine the organelles targeted by AtRabD1.

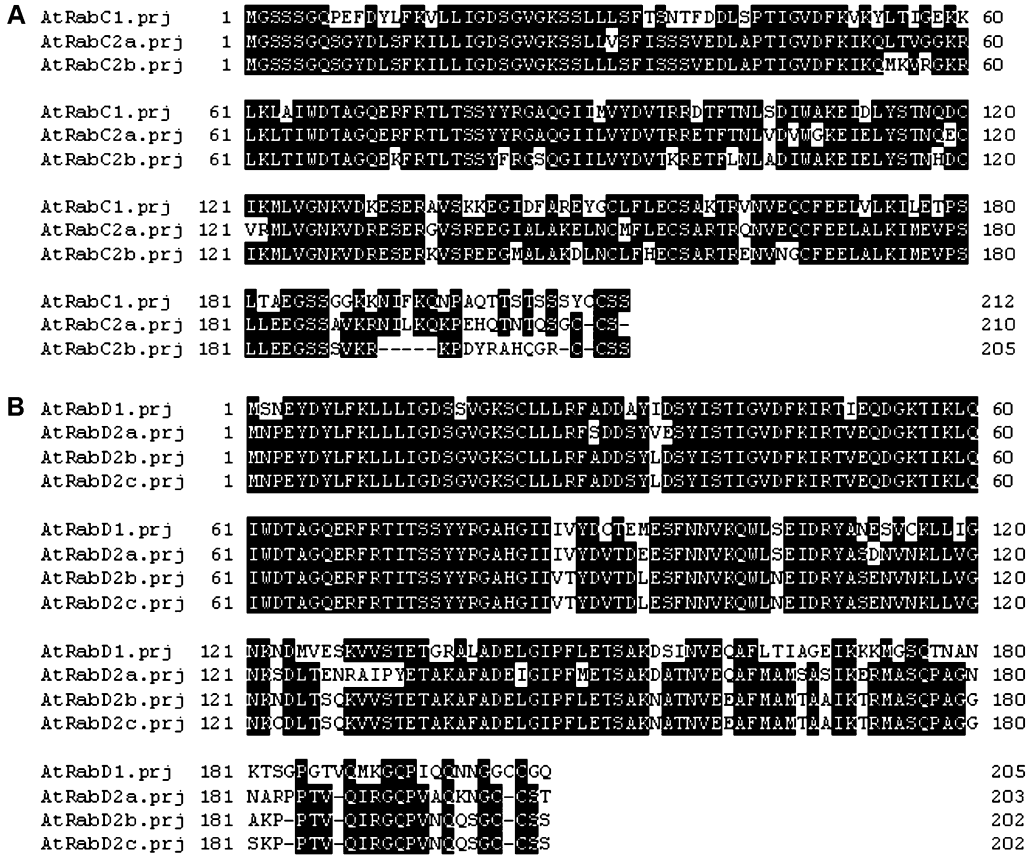

Fig. 5. Sequence comparison of AtRab protein isoforms in subgroup C (A) or D (B). Amino acids identical between at least two and three AtRab proteins in subgroup C (A) and D (B), respectively, are shown with a black background.

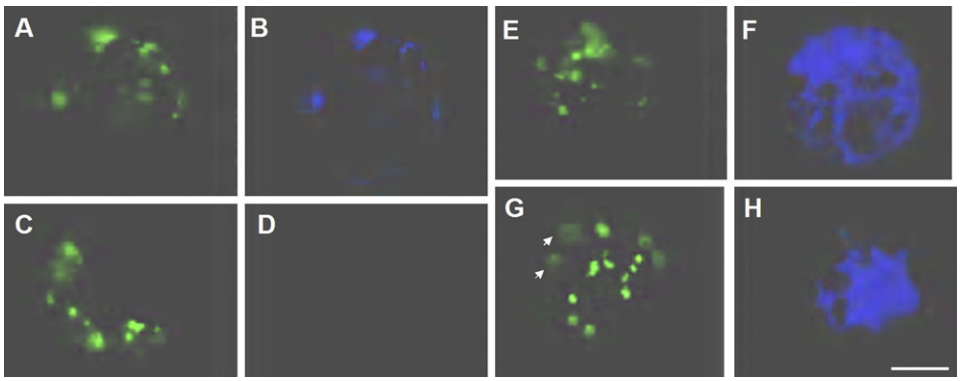

Fig. 6. Transient expression of CFP-tagged AtRab proteins in protoplasts stably expressing the GFP-tagged marker PTS1 for peroxisome. Protoplasts from *Arabidopsis* leaf tissue were transformed with CFP-tagged AtRabC2a (A, B) or AtRabD1 (E–H). After 16 h from the transformation, each signal was observed by a conventional fluorescent microscope. (A, C, E, G) Signals of GFP-tagged PTS1 corresponding to the localization of peroxisomes. (B) Signals of CFP-tagged AtRabC2a, and (F) and (H) are AtRabD1. White arrows indicate peroxisomes not overlapping with signals of AtRabD1 in (H). (D) An image of a protoplast not transformed with the CFP-tagged AtRabC2a, and acquired through a filter for CFP. Bar = 10 μm.

Discussion

In the present study, small GTPase Rabs, AtRabD1 and AtRabC2a, were identified as interacting factors with the MYA2 tail using the yeast two-hybrid screening method. Both recombinant AtRab proteins interacted with recombinant MYA2 tail protein in a GTP-dependent manner. However, the regions in the MYA2 tail important for the interaction with each AtRab were different between isoforms. Furthermore, it was found that CFP-tagged AtRabC2a expressed transiently in *Arabidopsis* leaf cells was co-localized with the peroxisome. Based on the evidence and results, it is suggested that the MYA2 is targeted to peroxisomes through the interaction with AtRabC2a.

In animal cells and yeast, Rab proteins play a role as an adaptor/receptor for myosin V, and are involved in targeting myosin V to the proper organelles and vesicles. For example, Myo2p of budding yeast (Itoh *et al*., 2002), myosin Vb (Lapierre *et al*., 2001; Hales *et al*., 2002), and myosin Va (Storm *et al*., 2002; Kuroda *et al*., 2003) of mammalian cells interact with the Rab protein, Ypt11p, Rab11 family proteins, and Rab27a, respectively, either directly or indirectly with other proteins to exert functions such as mitochondrial distribution, plasma membrane recycling, and normal melanosome transport. Recently, ATM1, a plant specific myosin VIII isoform, was shown to be co-localized with vesicles decorated with GFP-tagged Ara6 (Golomb *et al*., 2008), which is a plant Rab5 orthologue and regulates endocytosis in *Arabidopsis* cells (Ueda *et al*., 2001, 2004). Although the direct interaction of ATM1 with Ara6 *in vivo* or *in vitro* has not been examined, it was attractive to consider that myosin VIII is also associated with the AtRab protein, Ara6, on endocytotic vesicles.

Each AtRab had different MYA2 tail regions necessary for their interactions; AtRabC2a for both N- and C-termini in the tail. In a similar way in which the MYA2 tail interacts with AtRabC2a, mammalian myosin Vb tails interact with Rab11 family proteins, such as Rab11a, Rab11b, and Rab25 (Lapierre *et al*., 2001). The tail of mammalian myosin Vb, in which the coiled-coil domain is not contained, is able to interact directly with Rab11 family proteins. Using the yeast two-hybrid screening method and its truncated forms, two interaction sites in the myosin Vb tail are indicated. One site is Leu-Glu-Lys-Asn-Glu (LEKNE; N-site) located in the N-terminus (aa1421–aa1425), and the other is Leu-Leu-Leu-Asp (LLLD; C-site) in the C-terminus (aa1849–aa1852). A similar sequence to the N-site was not found in the N-terminal region of the MYA2 tail (data not shown). Surprisingly, however, Phe-Lue-Lue-Asp (FLLD) corresponding to LLLD of the C-site was present within 55 amino acids in the C-terminus of not only the MYA2 tail, but also other *Arabidopsis* myosin XI isoforms (Fig. 7), with the

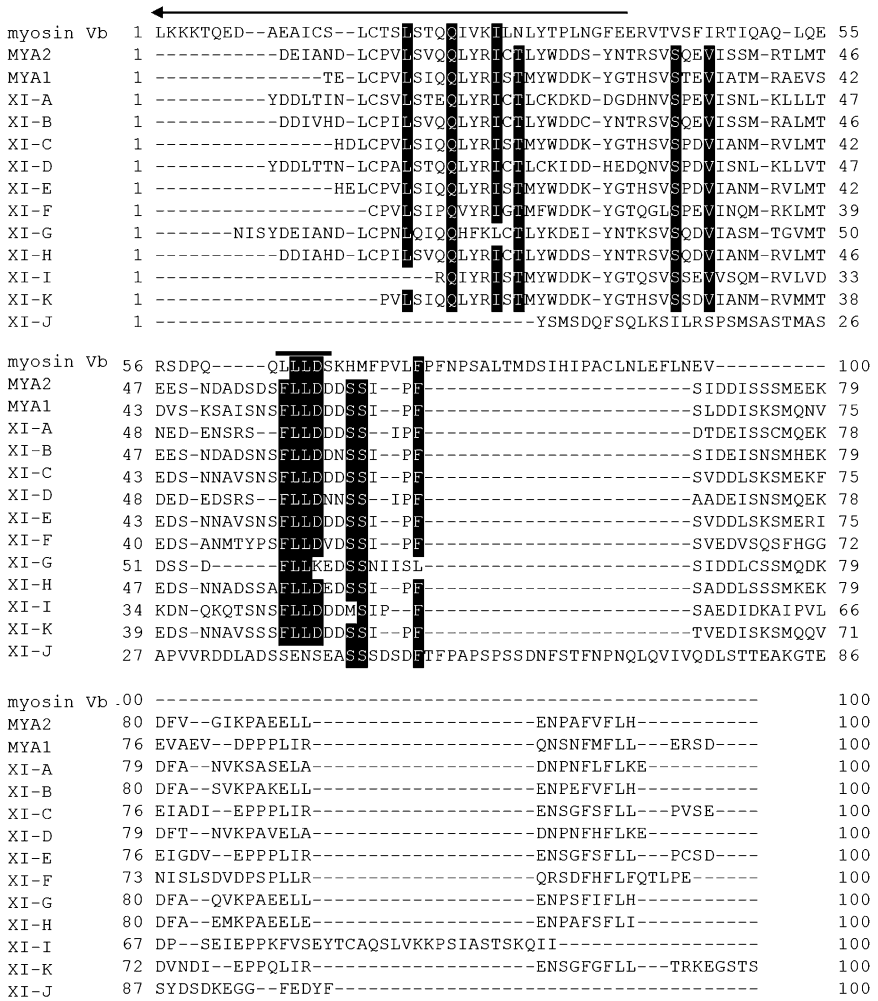

Fig. 7. Sequence comparison of 100 amino acids in the C-terminus of rat myosin Vb (myosin Vb) with those of *Arabidopsis* myosin XI (MYA2 to XI–J). Amino acids identical between 13 and 10 myosins are shown with a black background. An amino acid sequence, LLLD, required for association of myosin Vb with Rab11 family proteins is indicated by a black bar. An arrow indicates the C-terminal portion of the dilute domain.

exception of myosin XI-G and XI-J. In the case of XI-G, the last amino acid Asp in the four amino acid sequence was substituted with Lys (K). This conserved sequence was considered to play an important role in the interaction of myosin XI with AtRab proteins. The sequence was not included in a dilute domain (arrow in Fig. 7), which had been deduced to be necessary for cargo binding of myosin V (Reck-Peterson *et al*., 2000), but whose exact role has not yet been clarified.

The importance of both N- and C-termini of the MYA2 tails for interacting with AtRabC2a has been indicated, and it is suggested that MYA2 is targeted to the peroxisome through this interaction. However, a subdomain 2GT2, a C-terminal half spanning from aa1283 to aa1505 in the MYA2 tail, possessed a binding ability to the peroxisome (Li and Nebenfuhr, 2007). This result was contradictory to our suggestion, because the deleted fragment f4 (aa1195–aa1505) of the MYA2 tail containing the 2GT2 subdomain did not interact with AtRabC2a in the yeast two-hybrid screening assay. At present, this discrepancy cannot be explained. The subdomain 2GT2 might be targeted to the peroxisome without interacting with AtRabC2a, but by other mechanisms. Li and Nebenfuhr (2007) reported that a full-length MYA2 tail (MYA2GT, aa1091–aa1505) containing both 2GT1, a N-terminal half, and 2GT2 subdomains could not be targeted to the peroxisome or unknown organelles, suggesting that targeting and binding to organelles of myosin XI is tightly regulated in the cells. Conversely, Reisen and Hanson (2006) found that a MYA2 (myosin XI-6) tail (no coil, aa1053–aa1505) is targeted to the peroxisome when it was expressed in tobacco leaves. It is suggested that the N-terminus, aa1049–aa1195 in the MYA2 tail is necessary for interacting with AtRabC2a. Non-targeted MYA2 tail (MYA2GT) to the peroxisome started from aa1091, while the targeted tail (no coil) started from aa1053. This raises the possibility that the interacting site in the N-terminus of the MYA2 tail with AtRabC2a locates between aa1053 and aa1091, and that MYA2 tails with the site are able to interact with the peroxisome.

In the pull-down assay, the GTP-dependent interaction of both AtRab proteins with MYA2 tails *in vitro* appeared to be weak. The AtRab proteins bound to MYA2 tails were gradually dissociated from them by washing. The binding intensity or affinity of myosin V to the Rab protein has not been evaluated, because the interaction was examined by the yeast two-hybrid screening or an immunoprecipitation assay using cell lysate. In the latter case, there was a possibility that the interaction of myosin V with Rab protein is modified by other factors. Therefore, the intensity of interaction of MYA2 tail with AtRab proteins could not be compared to that of the myosin V tail with Rab proteins. As described above, Li and Nebenfuhr (2007) demonstrated the complicated behaviour of the MYA2 tail and its fragments having different domain lengths and suggested the presence of a mechanism for selection of the organelles which MYA2 binds to in the cells. Other myosin XI isoforms, such as MYA1, myosin XI-I, and myosin XI-K, showed similar behaviour to MYA2. Li and Nebenfuhr (2007) proposed the following model for explaining the selection mechanism of myosin XI. Subdomains, GT1 and GT2 can take on dynamically alternating conformations in the myosin XI tail. Initially, the tail binds to or interacts weakly with an organelle-specific adaptor, and selects one of these conformations, and then is locked effectively on to the organelle. According to this model, the weak interaction of the tail with the adaptor is one of the key events. Although it was not confirmed whether or not the weak interaction of MYA2 with AtRabC2a occurs in cells, our data might be consistent with and support the model. Alternatively, the possibility was considered that other factor(s), such as Rab11-FIP2 for the interaction of Rab11a with myosin Vb in mammalian cells (Hales *et al*., 2002), further regulates and modulates the interaction of AtRab proteins with the MYA2 tail. Hence, further study is needed to elucidate and confirm these points and possibilities, in addition to clarifying the location and function of AtRabD1.

Acknowledgement

This work was supported by a Grant-in Aid for Scientific Research on Priority Areas (Grant No. 17051026) to EY from the Ministry of Education, Culture, Spots, Science and Technology, Japan.

References

Ali BR, Seabra MC. 2005. Targeting Rab GTPases to cellular membranes. *Biochemical Society Transactions* **33,** 652–656.

Avisar D, Prokhnevsky AI, Makarova KS, Koonin EV, Dolja VV. 2008. Myosin XI-K is required for rapid trafficking of Golgi stacks, peroxisomes, and mitochondria in leaf cells of *Nicotiana benthamiana*. *Plant Physiology* **146,** 1098–1108.

Boevink P, Oparka K, Cruz SS, Martin B, Betteridge A, Hawes C. 1998. Stacks on tracks: the plant Golgi apparatus traffics on an actin/ER network. *The Plant Journal* **15,** 441–447.

Collings DA, Harper JDI, Vaughn KC. 2003. The association of peroxisomes with the developing cell plate in dividing onion root cells depends on actin microfilaments and myosin. *Planta* **218,** 204–216.

Foth BJ, Goedecke MC, Soldati D. 2006. New insight into myosin evolution and classification. *Proceedings of the National Academy of Sciences, USA* **103,** 3681–3686.

Golomb L, Abu-Abied M, Belausov E, Sadot E. 2008. Different subcellular localization and functions of Arabidopsis myosin VIII. *BMC Plant Biology* **8,** 1–13.

Hales CM, Vaerman JP, Goldenring JR. 2002. Rab11 family interacting protein 2 associates with myosin Vb and regulates plasma membrane recycling. *Journal of Biological Chemistry* **277,** 50415–50421.

Hashimoto K, Igarashi H, Mano S, Nishimura M, Shimmen T, Yokota E. 2005. Peroxisomal localization of a myosin XI isoform in *Arabidopsis thaliana*. *Plant and Cell Physiology* **46,** 782–789.

Higaki T, Kutsuna N, Okubo E, Sano T, Hasezawa S. 2006. Actin microfilaments regulate vacuolar structures and dynamics: dual observation of actin microfilaments and vacuolar membrane in living tobacco BY-2 cells. *Plant and Cell Physiology* **47,** 839–852.

Itoh T, Watabe A, Toh EA, Matsui Y. 2002. Complex formation with Ypt11p, a rab-type small GTPase, is essential to facilitate the fnction of Myo2p, a class V myosin, in mitochondrial distribution in *Saccharomyces cerevisiae*. *Molecular and Cellular Biology* **22,** 7744–7757.

Jedd G, Chua NH. 2002. Visualization of peroxisomes in living plant cells reveals acto-myosin-dependent cytoplasmic streaming and peroxisome budding. *Plant and Cell Physiology* **43,** 384–392.

Kuroda TS, Ariga H, Fukuda M. 2003. The actin-binding domain of Slac2-a/melanophilin is required for melanosome distribution in melanocytes. *Molecular and Cellular Biology* **23,** 5245–5255.

Kwok EY, Hanson MR. 2003. Microfilaments and microtubules control the morphology and movement of non-green plastids and stromules in *Nicotiana tabacum*. *The Plant Journal* **35,** 16–26.

Laemmli UK. 1970. Cleavage of structural proteins during the assembly of the head of bacteriophage T4. *Nature* **227,** 680–685.

Lapierre LA, Kumar R, Hales CM, Navarre J, Bhartur SG, Burnette JO, Provance Jr DW, Mercer JA, Bahler M, Goldenring JR. 2001. Myosin Vb is associated with plasma membrane recycling systems. *Molecular Biology of the Cell* **12,** 1843–1857.

Li J-F, Nebenfuhr A. 2007. Organelle targeting of myosin XI is mediated by two globular tail subdomains with separate cargo binding sites. *Journal of Biological Chemistry* **282,** 20593–20602.

Logan DC, Leaver CJ. 2000. Mitochondria-targeted GFP highlights the heterogeneity of mitochondrial shape, size and movement within living plant cells. *Journal of Experimental Botany* **51,** 865–871.

Mano S, Nakamori C, Hayashi M, Kato A, Kondo M, Nishimura M. 2002. Distribution and characterization of peroxisomes in *Arabidopsis* by visualization with GFP: dynamic morphology and actin-dependent movement. *Plant and Cell Physiology* **43,** 331–341.

Mathur J, Mathur N, Hulskamp M. 2002. Simultaneous visualization of peroxisomes and cytoskeletal elements reveals actin and not microtubule-based peroxisome motility in plants. *Plant Physiology* **128,** 1031–1045.

Nebenfuhr A, Gallagher L, Dunahay TG, Frohlick JA, Mazurkiewicz AM, Staehelin LA. 1999. Stop-and-go movements of plant Golgi stacks are mediated by the acto-myosin system. *Plant Physiology* **121,** 1127–1141.

Paves H, Truve E. 2007. Myosin inhibitors block accumulation movement of chloroplasts in *Arabidopsis thaliana* leaf cells. *Protoplasma* **230,** 165–169.

Peremyslov VV, Prokhnevsky AI, Avisar D, Dolja VV. 2008. Two class XI myosins function in organelle trafficking and root hair development in Arabidopsis. *Plant Physiology* **146,** 1109–1116.

Reck-Peterson SL, Provance Jr DW, Mooseker MS, Mercer JA. 2000. Class V myosins. *Biochimica et Biophysica Acta* **1496,** 36–51.

Reddy ASN, Day IS. 2001. Analysis of the myosins encoded in the recently completed *Arabidopsis thaliana* genome sequence. *Genome Biology* **2,** research0024.

Reichelt S, Kendrick-Jones J. 2000. Myosins. In: Staiger CJ, Baluska F, Volkmann D, Barlow PW, eds. *Actin: dynamic framework for multiple plant cell functions*. Dordrecht: Kluwer Academic Publisher, 29–44.

Reisen D, Hanson MR. 2006. Association of six YFP-myosin XI-tail fusions with mobile plant cell organelles. *BMC Plant Biology* **7,** 1–17.

Romagnoli S, Cai G, Faleri C, Yokota E, Shimmen T, Cresti M. 2007. Microtubule- and actin filament-dependent motors are distributed on pollen tube mitochondria and contribute differently to their movement. *Plant and Cell Physiology* **48,** 345–361.

Sellers JR. 2000. Myosins: a diverse superfamily. *Biochimica et Biophysica Acta* **1496,** 3–22.

Storm M, Hume AN, Tarafder AK, Barkagianni E, Seabra MC. 2002. A family of Rab27-binding proteins: melanophilin links Rab27a and myosin Va function in melanosome transport. *Journal of Biological Chemistry* **277,** 25423–25430.

Ueda T, Uemura T, Sato MH, Nakano A. 2004. Functional differentiation of endosomes in *Arabidopsis* cells. *The Plant Journal* **40,** 783–789.

Ueda T, Yamaguchi M, Uchimiya H, Nakano A. 2001. Ara6, a plant-unique novel type Rab GTPase, functions in the endocytic pathway of *Arabidopsis thaliana*. *EMBO Journal* **20,** 4730–4741.

Van Gestel KV, Kohler RH, Verbelen J-P. 2002. Plant mitochondria move on F-actin, but their positioning in the cortical cytoplasm depends on both F-actin and microtubules. *Journal of Experimental Botany* **53,** 659–667.

Wada M, Kagawa T, Sato Y. 2003. Chloroplast movement. *Annual Review of Plant Biology* **54,** 455–468.

Wang Z, Pesacreta TC. 2004. A subclass of myosin XI is associated with mitochondria, plastids, and the molecular chaperone subunit TCP-1α in maize. *Cell Motility and the Cytoskeleton* **57,** 218–232.